# Electrochemical Deposition of Uranium Oxide

# in Highly Concentrated Calcium Chloride

Akihiro Uehara [a*], Osamu Shirai [b], Toshiyuki Fujii [a],

Takayuki Nagai [c], Hajimu Yamana [a]

[a] *Division of Nuclear Engineering Science, Research Reactor Institute, Kyoto University,*

*Asashironishi, Kumatori, Osaka,590-0494, Japan*

[b] *Division of Applied Life Sciences, Graduate School of Agriculture, Kyoto University,*

*Sakyo, Kyoto, 606-8502, Japan*

[c] *Nuclear Fuel Cycle Engineering Lab., Japan Atomic Energy Agency, 4-33,*

*Muramatsu, Tokai, Naka, Ibaraki 319-1194, Japan*

---

**Abstract**

The coordination circumstances and redox reactions of $UO_2^{2+}$ in the aqueous solution concentrated by calcium chloride such as $CaCl_2 \cdot 6H_2O$ (6.9 M $CaCl_2$) were studied by Raman spectroscopy and electrochemical methods.   The frequency of the O=U=O symmetrical stretching vibration suggested that the complex formation of $UO_2^{2+}$ with $Cl^-$ leads to the weakening of U=O bond.   In the electrochemical measurements, two step cathodic currents were observed at −0.090 and −0.4 V (vs. Ag|AgCl) corresponding to the reduction of $UO_2^{2+}$ to $UO_2^+$ and that of $UO_2^+$ to $UO_2$, respectively.   It was found that $UO_2^+$ formed at first cathodic current was disproportionated to form $UO_2^{2+}$ and $UO_2$. The $UO_2$ was identified by X-ray diffraction analysis.   Electrolytic deposition of $UO_2$

was observed in 6.9 – 4.7 M $CaCl_2$ and in 14 M LiCl. When small amount of proton *i.e.*, 0.005 M was coexisted in 6.9 M $CaCl_2$, $UO_2^{2+}$ was reduced to form $U^{4+}$ instead of $UO_2$.

---

*Keywords: Calcium chloride, Hydrate melt, Uranium oxide, Deposit, Voltammetry, Ramman spectroscopy.*

\* Author to whom correspondence should be addressed

  E-mail: auehara@rri.kyoto-u.ac.jp (A. Uehara)

TEL: +81-724-51-2454, FAX: +81-724-51-2634

## 1. Introduction

Pyrochemical dry reprocessing of spent nuclear fuels has been developed with the PUREX process. The pyrochemical reprocessing includes the dissolution of spent nuclear fuels in a molten salt medium and the selective recovery of actinides. In traditional, these inorganic molten salts, act as electrolytes, are composed of an eutectic of several alkali or alkaline earth chlorides, melt at temperature above 800 K [1,2] depending upon the composition of the chosen eutectic. Therefore, handling difficulties or significant damages of equipment and materials have been concerned. Recently, room temperature ionic liquids (RTILs) such as 1-butyl-3-methylimidazolium chloride were introduced into the dry reprocessing of the spent nuclear fuel instead of high temperature molten salts. Giridhar *et al.* [3] and Asanuma *et al.* [4] reported that uranium was recovered by the electrochemical reduction of $UO_2^{2+}$ on the cathode. However, radiolysis of ionic liquids due to the fission products should be taken into account. On the other hand, it has been also reported that the deposition of uranium oxide was formed electrochemically in very weak acid aqueous solution [5].

Calcium chloride hexahydrate, $CaCl_2 \cdot 6H_2O$, and similar hydrates which are highly concentrated electrolytes (6.9 M $CaCl_2$) have low melting points and can be used as solutions. The chemical properties of their hydrates are intermediate between aqueous solutions and molten salts. By considering enthalpies of dissolution [6], activity coefficients [7], vapor pressure [8] and their structural analyses [9,10], it is assumed that the water molecules in $CaCl_2 \cdot 6H_2O$ melts are strongly coordinated to calcium ion showing that this melt is a liquid with the properties of an ionic melt composed of bulky

hydrated cations and chloride anions. According to X-ray absorption fine structure analyses, U(VI) species in 6.9 M $CaCl_2$ were estimated to be $UO_2Cl_2(H_2O)_2$ [11] which was distinctly different from $[UO_2(H_2O)_5]^{2+}$ in 0.1 M $HClO_4$. There are a few studies of the electrochemistry for the redox of $UO_2^{2+}$ in the aqueous solution concentrated by the electrolytes [12-14]. Cohen [12] reported that the formation of $UO_2^+$ in the aqueous solution highly concentrated by $CaCl_2$ and LiCl was identified absorption spectrophotometrically.   He has also reported that uranium compounds were deposited on the cathode by electrolysis.   Bansal et al. [13,14] reported that $UO_2^{2+}$ was readily reduced to $UO_2^+$, and that was further reduced to $UO_2$ in the calcium nitrate terahydrate, $Ca(NO_3)_2 \cdot 4H_2O$, melt. However, the deposited compounds could not be identified since these compounds were very oxidative.

In the present study, the coordination circumstance and the redox reaction of $UO_2^{2+}$ in the highly concentrated $CaCl_2$ solution are investigated based on Raman spectroscopy and cyclic voltammetry.   Then uranium oxide is recovered as an electro-deposit by the controlled potential electrolysis.   The mechanism of the reduction of $UO_2^{2+}$ is discussed electrochemically and spectrophotometrically.   Potential-controlled electrolysis was carried out in various kinds of electrolyte solutions to define the conditions for $UO_2$ deposition.

## 2. Experimental

Calcium chloride hexahydrate, $CaCl_2 \cdot 6H_2O$, of analytical grade (Fluka Co.) was

used after filtration. Uranyl chloride, $UO_2Cl_2$ hydrate, was prepared by evaporating aqueous solution of $UO_2Cl_2$ and HCl. The $H_3O^+$ remained in the salt was less than 1%, which was calculated by pH measurement after solid was dissolved in a certain amount of water. The concentration of uranium ion was determined based on the absorption spectroscopy [15]. A self-registering spectrophotometer V-350 (JASCO Co.) and UV-1000 (Shimadzu Co.) was used for the measurements over the wavelength from 350 to 1700 nm. Raman spectra were obtained an excitation using the 514.5 nm line of $Ar^+$ laser (NEC, GLS3280 and GLG3280). The laser power at the sample was 300 mW. The Raman scattering was collected at $90^o$ to the incident beam. The Raman spectra were recorded by a JASCO NR-1100 spectrometer at 0.1 $cm^{-1}$ interval. The scanning rate was 60 $cm^{-1}$ $min^{-1}$. One hundred scans for one sample in the range from $800 - 900\ cm^{-1}$ were averaged to obtain the final spectrum. The measurements were performed at ambient temperature of $293 - 295$ K, and no evidence of warming was observed.

For the electrochemical measurements, a three-electrode system was used. A glassy carbon rod (Tokai Carbon Co.) of 5 mm $\phi$ or platinum rod (Nilaco Co.) of 2 mm $\phi$ was used as a working electrode, and the silver|silver chloride (Ag|AgCl) electrode was used as a reference electrode. This reference electrode consists of an end-closed tube by glass filter, in which aqueous solution containing 1 M LiCl was put in with a Ag wire of 1 mm diameter coated by AgCl. For every electrochemical experiment, the platinum mesh electrode was employed as a counter electrode. An electrochemical measurement system, Hz-5000 (Hokuto Denko Co.) was used for the cyclic voltammetry.

In order to identify the electrode reaction, controlled potential electrolysis was

carried out.    In this experimental, a platinum mesh electrode was employed as a working electrode to enhance the efficiency of the electrolysis.    The counter electrode was also platinum mesh electrode, counter phase was separated by glass filter membrane from the objective phase to avoid cyclic redox reaction.    After controlled potential electrolysis, absorption spectra were measured.    When an electrodeposit was obtained by the electrolysis, the deposit was separated by PTFE membrane filter and washed by ethanol.    The deposit was dried up under the air condition and was analyzed by X-ray diffraction method with RINT-2100 diffractometer (Rigaku Co.) using Cu Kα radiation (40 kV, 40 mA).

These measurements were carried out at 298 K for cyclic voltammetry and at 332 K for and bulk electrolysis.

## 3. Results and discussion

### 3.1. Coordination of $UO_2^{2+}$ in 6.9 M $CaCl_2$

An absorption spectrum of $UO_2Cl_2$ in 6.9 M $CaCl_2$ was shown as curve 1 in Fig. 1. The molarabsorptivity was plotted as a function of wavelength in Fig. 1.    Clear four peaks were observed at 415, 428, 440 and 476 nm.    The molar absorptivity at 428 nm was 19.9, which is over twice larger than that obtained in 1 M $HClO_4$ as shown by curve 2 in Fig. 1 [15].    The charge transfer band was observed in the wavelength range less than 408 nm.    The absorption spectrum in 6.9 M $CaCl_2$ containing $UO_2Cl_2$ was

different from that in the aqueous solution containing uranyl hydrolysis or oligomer species reported by Quiles et al. [16]. The uranyl species in 6.9 M $CaCl_2$ does not form hydrolysis species even though $H^+$ was not coexistence with the melt.

Curve 1 in Fig. 2 shows the Raman spectrum of uranyl perchlorate dissolved in 1 M $HClO_4$. Here, 1M perchlorate solution was employed as a standard media so that the equatorial sphere of uranyl ion is coordinated by five water molecules. Under this condition, the uranyl complex is presented in the unhydrolyzed form. The band at 872 $cm^{-1}$ was previously assigned to be $\nu_1$ symmetrical stretching vibration of U=O bond [17,18]. When the Raman spectrum was measured by using 6.9 M $CaCl_2$ (curve 2), the $\nu_1$ shift was observed at 855.4 $cm^{-1}$ which was 16.6 $cm^{-1}$ lower energy than the shift obtained in 1 M $HClO_4$. This indicated that the coordination of $Cl^-$ in 6.9 M $CaCl_2$ affected the polarizability of U=O bond. Coordination number of $Cl^-$ to $UO_2^{2+}$ in concentrated $CaCl_2$ seems to be higher than that in LiCl at similar concentration of $Cl^-$ [19]. On the other hand, no difference was seen in the $\nu_1$ frequency between $Ca(NO_3)_2 \cdot 4H_2O$ (7.2 M Ca) and 1 M $HClO_4$ [20]. This suggested that the substitution of hydrated water molecule by $NO_3^-$ ion did not change the polarizability of U=O bond. Covalency (or electron donating ability) of O donors in hydrated water molecule and $NO_3^-$ may be similar in $Ca(NO_3)_2 \cdot 4H_2O$.

According to EXAFS analyses, uranyl species in 6.9 M $CaCl_2$ were estimated to be $UO_2Cl_2(H_2O)_2$ [11]. The similar complex was also formed in 14 M LiCl [21] but it was distinctly different from $[UO_2(H_2O)_5]^{2+}$ in 0.1 M $HClO_4$. Though the coordination number of $Cl^-$ determined by XAFS [21] seems to be lower than that determined by Raman spectroscopy [19], the first coordination sphere of $UO_2^{2+}$ is surrounded by a few

numbers of Cl$^-$ in 6.9 M CaCl$_2$.

*3.2. Electrochemical analysis for the redox reaction of UO$_2^{2+}$ in 6.9 M CaCl$_2$*

Figure 3 shows the voltammograms for the redox reaction of 0.05 M UO$_2$Cl$_2$ in 6.9 M CaCl$_2$ by using a platinum working electrode. When the potential scanning rate, *v*, was from 0.01 to 0.5 V s$^{-1}$, a cathodic peak current ($I_{c,1}$) was observed at −0.090 V (vs. Ag|AgCl) corresponding to the reduction of UO$_2^{2+}$ to UO$_2^+$ as Eq. (1);

$$UO_2^{2+} \ + \ e^- \ \rightleftarrows \ UO_2^+ \tag{1}$$

The $I_{c,1}$ was proportional to the square of *v* between 0.01 and 0.5 V s$^{-1}$ and the concentration of UO$_2^{2+}$ between $5 \times 10^{-3}$ and 0.06 M. These results indicated that the $I_{c,1}$ were controlled by the diffusion of UO$_2^{2+}$. An anodic peak current ($I_{a,1}$) was observed at 0.025 V (vs. Ag|AgCl) under the potential scanning rate from 0.1 to 0.5 V s$^{-1}$. Mid-point potential between cathodic and anodic peaks was found to be −0.058 V.   Assuming that the electrode reaction of the UO$_2^{2+}$|UO$_2^+$ couple is reversible, the diffusion coefficient of UO$_2^{2+}$ at 298 K can be calculated to be $1.7 \times 10^{-7}$ cm$^2$ s$^{-1}$, which was more 10 times smaller than that in diluted electrolyte solutions such as 0.1 M HClO$_4$ ($7.3 \times 10^{-6}$ cm$^2$ s$^{-1}$) [22]. On the other hand, at *v* < 0.1 V s$^{-1}$, anodic peak potential shifted positive from 0.025 to 0.165 V (vs. Ag|AgCl). This shift suggests that disproportionation of UO$_2^+$ occurs after the reduction of UO$_2^{2+}$ as following reaction [13];

8

$$2\,UO_2^+ \;\rightleftarrows\; UO_2^{2+} \;+\; UO_2 \tag{2}$$

The rate of disproportionation in 6.9 M CaCl$_2$ was estimated based on EC reaction undergoing Eqs. (1) and (2) to be 60 M$^{-2}$ s$^{-1}$ which was similar to that in 0.4 M HClO$_4$ [23]. The cyclic voltammograms were recorded at more negative potential than −0.2 V as shown in Fig. 4. Another cathodic current ($I_{c,2}$) around −0.4 V (vs. Ag|AgCl) was observed, scanning potential up to −0.5 V (vs. Ag|AgCl) as curve 5. The $I_{c,2}$ was estimated by the reduction of UO$_2^+$ to UO$_2$ as following Eq. (3);

$$UO_2^+ \;+\; e^- \;\rightleftarrows\; UO_2 \tag{3}$$

This reaction is observed in high temperature molten salts [24] and RTILs [4], but not in aqueous solutions containing diluted electrolytes. On the other hand, anodic peak currents shifted depended on the negative potential region swept from −0.16 to −0.6 V (vs. Ag|AgCl) as curves 3 to 5. Scanning potential up to −0.4 V (vs. Ag|AgCl) as curve 3, $I_{a,1}$ decreased, two anodic currents ($I_{a,2}$ and $I_{a,3}$) increased at 0.24 and 0.51 V (vs. Ag|AgCl), respectively. When the potential was scanned to −0.5 and −0.6 V (vs. Ag|AgCl) as curves 4 and 5, respectively, $I_{a,2}$ and $I_{a,3}$ were kept almost constant. Taken the disproportionation reaction as Eq. (2) and the reduction of UO$_2^+$ as Eq. (3) into account, those anodic reactions were estimated as follows;

$$UO_2 \;\rightleftarrows\; UO_2^{2+} \;+\; 2\,e^- \tag{4}$$

$$UO_2 \quad \rightleftarrows \quad UO_2^+ \quad + \quad e^- \tag{5}$$

Cyclic voltammograms depended on $v$ from 0.01 to 0.5 V s$^{-1}$ were observed at the potential region between $-0.5$ and 0.7 V (vs. Ag|AgCl) in Fig. 5. Cathodic and anodic peak currents depended on $v$. At $v = 0.01$ and 0.02 V s$^{-1}$, $I_{c,2}$ was not observed. However, at $v > 0.05$ V s$^{-1}$, second cathodic current increased with an increase in $v$. These results indicated that the concentration of $UO_2^+$ at the electrode surface decreased due to the disproportionation as Eq. (2) at $v < 0.02$ V s$^{-1}$.

*3.3. Determination of reduction reactions by potential-controlled electrolysis in 6.9 M CaCl$_2$*

In order to identify the reaction of $I_{c,2}$ observed at $-0.4$ V (vs. Ag|AgCl), the potential-controlled electrolysis was carried out by applying more negative potential than $-0.5$ V. the temperature of the solution phase was kept at 332 K to decrease the viscosity of the hydrate melt. The viscosity of the melt at 332 K was about twice lower than that at 298 K. Electrode potential was kept at $-0.6$ V (vs. Ag|AgCl), and the electrolysis was performed for about 12 hrs. After the electrolysis, the color of the solution changed from yellow to black. When the black solution was left for one day, the black compounds precipitated on the surface of the platinum mesh working electrode and on the bottom of vessel. On the other hand, the bulk solution appeared to be clear and colorless. It was found that the compound obtained in this study was not oxidized in CaCl$_2 \cdot 6H_2O$ at least more than two weeks, and any absorption peaks

corresponding to uranium ions such as $UO_2^{2+}$ and $U^{4+}$ [25] in $CaCl_2 \cdot 6H_2O$ were not observed. After the deposit was filtered, it was washed by ethanol and was dried up. Figure 6 shows deposit compounds. When SEM was performed, particle size of the deposition as shown in Fig. 7 (a) was smaller than that of $UO_2$ crystal as shown in Fig. 7 (b). When the XRD analysis was carried out by using those compounds, the result of the electro-deposit and $UO_2$ crystal were shown as curves 1 and 2, respectively, in Fig. 8. The asterisk * indicates the peak of $UO_2$ crystal based on the database [26]. These peaks in curve 1 gave close agreement with that of the database. However, it was found that the electro-deposit was not fine crystalline form because those compounds were mainly formed by disproportionation of $UO_2^+$. The percent yield of the uranium oxide calculated based on the weight of the deposit was found to be more than 85%. Consequently, it was found that the reaction at $I_{c,2}$ was attributable to the deposition of $UO_2$. Electrolytic deposition was performed in concentrated $CaCl_2$ by Cohen *et al.*[12], however, they did not identified the compounds because the compound obtained by centrifuge was re-oxidized. In this study, however, by filtration and washing with ethanol, it was found that the product was not oxidized at least for a week. Bansal *et al.* [13] reported that the reaction at the second cathodic current at $-0.4$ V corresponded to the formation of $UO_2$ from $UO_2^+$ in $Ca(NO_3)_2 \cdot 4H_2O$ melt as Eq. (3). They observed the deposit on the electrode surface.

Assuming that the reduction proceeds based on the Eq. (2), the deposit corresponding to the formation of $UO_2$ on $I_{c,1}$ would be observed. To confirm the process corresponding to Eq. (2), the following procedures were duplicated for 9 times; the electrolysis was carried out for an hour by applying a constant potential, the

11

absorption spectrum was measured after the electrolysis. The result was shown in Fig. 9. When –0.05 V was applied for 0.5 h, the absorption peaks corresponding to $UO_2^+$ at wide wavelength between 500 – 1300 nm and a peak at 1510 nm were observed [12]. The absorption peaks increased with progress of the controlled potential electrolysis, however the black deposit of $UO_2$ was observed on the electrode surface and in the bulk solution. After the controlled potential electrolysis procedure, the absorption peak of the $UO_2^+$ decreased. These results indicated that $UO_2^+$ formed by the electrochemical reduction was spontaneously converted to $UO_2^{2+}$ and $UO_2$ by disproportionation based on the Eq. (2).

*3.4. Electrolytic deposition in various kinds of electrolyte solutions*

The potential-controlled electrolysis was carried out in various kinds of electrolyte solutions to define the conditions for $UO_2$ deposition. Dependences of the water content in $CaCl_2 \cdot RH_2O$ ($R$ = 6, 7, 8, 9, 10 and 15), of which concentration of $CaCl_2$ were 6.9, 6.2, 5.6, 5.1, 4.7, and 3.3 M, respectively, were examined. Cyclic voltammograms were recorded in each melt containing $UO_2Cl_2$ as shown in Fig. 10. Peak currents increased and peak potential shifted negative with an increase in the water content. This is because the viscosity of $CaCl_2$ solutions decreases with an increase in the water content. It was found that the deposition of $UO_2$ was attained in the concentration range from 6.9 to 4.7 M $CaCl_2$ by the electrolysis experiments without argon bubbling. Since the deposit in 4.7 M $CaCl_2$ was not stable, the compounds were re-oxidized to form $UO_2^{2+}$ less than a week. Using 3.3 M $CaCl_2$, $UO_2$

was formed only on the surface of the electrodes and re-oxidized a few hours later. Hydrolysis species such as $UO_2(OH)^+$ and $UO_2(OH)_2$ were formed according to the results of the absorption spectra. Similar behavior has been observed in 0.01 M HCl which is weakly acidic solutions [5] though the deposit can be obtained by the electrolysis under argon gas atmosphere.

The deposition experiment in 14 M LiCl was also carried out. Here, the concentration of $Cl^-$ in 14 M LiCl was similar to that in 6.9 M $CaCl_2$. The cyclic voltammogram of $UO_2Cl_2$ in 14 M LiCl shows similar results obtained in 6.9 M $CaCl_2$. The $UO_2$ deposit was obtained by potential-controlled electrolysis. This is because $UO_2^{2+}$ in 14 M LiCl is coordinated by $Cl^-$ instead of $H_2O$, actually the coordination number of $Cl^-$ to $UO_2^{2+}$ in 14 M LiCl is larger than that in 6.9 M $CaCl_2$ [11].

The effect of $H^+$ in concentrated $CaCl_2$ solution on the electrolysis was examined in 6.9 M $CaCl_2$ and 0.025 M $UO_2Cl_2$ coexisted with 0.005 M HCl. When the cyclic voltammogram was recorded, cathodic peak current was observed at −0.09 V corresponding to the reduction of $UO_2^{2+}$. However, reduction products were not $UO_2$ deposits but tetravalent cation of U, $U^{4+}$, resulted from absorption spectra of bulk solution. This reaction is observed in acidic aqueous solutions as Eq. (6);

$$2\,UO_2^+ \;+\; 4\,H^+ \;\rightleftharpoons\; UO_2^{2+} \;+\; U^{4+} \;+\; 2\,H_2O \tag{6}$$

The $UO_2^+$ formed by the electroreduction of $UO_2^{2+}$ rapidly converted to $UO_2^{2+}$ and $U^{4+}$ by the disproportionation based on the Eq. (4). It was known that activity coefficient of $H^+$ was over 10 in concentrated electrolyte solutions. Therefore, it was

suggested that small amount of $H^+$ in $CaCl_2$ hydrate melt disturbed the deposition of $UO_2$ from formation of $UO_2Cl_2$ by the electrolysis.

It was found that these reactions occurring in $CaCl_2$ melt were different from those occurring in neutral [5] aqueous solutions as Eq. (7), respectively.

$$2\,UO_2^+ \;+\; H^+ \;\rightleftarrows\; UO_2(OH)^+ \;+\; UO^{2+} \tag{7}$$

In the reduction of $UO_2^{2+}$ on a platinized platinum electrode under certain conditions (274 K, pH = 2.5 − 3.0, uranium concentration $1 \times 10^{-3}$ M) up to 90% of $UO_2^+$ could be obtained [5], then $UO_2^+$ disproportionated with the formation of $UO_2(OH)^+$ and $UO^{2+}$ as Eq. (7). According to the Eqs. (6) and (7), $H^+$ is concerned with the reduction of $UO_2^{2+}$ in these solutions.   On the other hand, $H_2O$ in hydrate melts did not dissociate to form free $H^+$ because the hydration with $Ca^{2+}$ was more effective than the dissociation of $H_2O$.

## 4.   Conclusion

The reduction of $UO_2^{2+}$ in highly concentrated $CaCl_2$ and $LiCl$ was investigated based on cyclic voltammetry and controlled potential electrolysis.   Mid-point potential for the redox of the $UO_2^{2+}|UO_2^+$ couple determined to be −0.058 V (vs. Ag|AgCl).   The $UO_2^+$ formed by the electroreduction of $UO_2^{2+}$ was converted spontaneously to form both $UO_2^{2+}$ and $UO_2$ by the disproportionation of $UO_2^+$.   It was found that $UO_2$ deposit

was obtained by the electrolysis in highly concentrated $CaCl_2$ (> 4.7 M) and LiCl at room temperature without nitrogen substitution, since $Cl^-$'s coordinate equatorial sphere of $UO_2^{2+}$ resulted in avoiding the hydrolysis. However, $UO_2^{2+}$ was easily reduced to $U^{4+}$ when lower concentration of $H^+$ than $UO_2^{2+}$ existed in the concentrated electrolytes.

**Acknowledgement**

**References**

[1]     J.L. Willit, W.E. Miller, J.E. Battles, J. Nucl. Matr. 195 (1992) 229.

[2]     G.R. Choppin, A. Morgenstern, J. Radioanal. Nucl. Chem. 243 (2000) 45.

[3]     P. Giridhar, K.A. Venkatesan, T.G. Srinivasan, P.R. Vasudeva Rao, Electrochim. Acta 52 (2007) 3006.

[4]     N. Asanuma, M. Harada, Y. Yasuike, M. Nogami, K. Suzuki, Y. Ikeda, J. Nucl. Sci. Technol. 44 (2007) 368.

[5]     W.E. Harris and I.M. Kolthoff, J. Am. Chem. Soc., 69 (1947) 446.

[6]     G.C. Sinke, E.H. Mossner, J.L. Curnutt, J. Chem. Thermodynamics 17 (1985) 893.

[7]     J.A. Rard, S.L. Clegg, J. Chem. Eng. Data 42 (1997) 819.

[8]     G.G. Aseyev, Electrolytes: Equilibria in solutions and phase equilibria, Begell house Inc.1999.

[9]     A.A. Chialvo, J.M. Simonson, J. Chem. Phys. 119 (2003) 8052.

[10]    T. Yamaguchi, S. Hayashi, H. Ohtaki, Inorg. Chem., 28 (1989) 2434.

[11]    A. Uehara, T. Fujii, H. Matsuura, N. Sato, H. Yamana, Y. Okamoto, OECD-NEA, 15 (2009) 197.

[12]    D. Cohen, J. Inorg. Nucl. Chem. 32 (1970) 3525.

[13]    N.P. Bansal, J.A. Plambeck, Electrochim. Acta, 23 (1978) 1053.

[14]    N.P. Bansal, J.A. Plambeck, Can. J. Chem., 59 (1981) 1515.

[15]    D.M. Gruen, R.L. McBeth, J. Inorg. Nucl. Chem. 9 (1959) 290.

[16]    F. Quiles, C. Nguyen-Trung, C. Carteret, B. Humbert, Inorg. Chem., 50 (2011) 2811.

[17]    L.M. Toth, G.M. Begun, J. Phys. Chem. 85 (1981) 547.

[18]    M. Asano, J.A. Koningstein, Can. J. Chem. 60 (1982) 2207.

[19]    C. Nguyen-Trung, G.M. Begun. and D.A. Palmer, Inorg. Chem., 31 (1992) 5280.

[20]    T. Fujii, H. Yamana, H. Moriyama, J. Nucl. Sci. Technol. Suppl. 3(2002) 336.

[21]    P.G. Allen, J.J. Bucher, D.K. Shuh, N.M. Edelstein, and T. Reich, Inorg. Chem., 36 (1997) 4676.

[22]     A.P. Vinogradov Ed. Analytical Chemistry of Uranium, Academy of Sciences,

         Moskva, 1962, p. 144.

[23]     R.T. Iwamoto, J. Am. Chem. Soc., 63 (1959) 303.

[24]     I. Uchida, J. Nikura, S. Toshima, J. Electroanal. Chem., 124 (1981) 165.

[25]     A. Uehara, T. Fujii, T. Nagai, O. Shirai, N. Sato, H. Yamana, Recent Advances

         in Actinide Science, I. May, R. Alvares, N. Bryan Eds. pp. 548-550 (2006).

[26]     Powder diffraction file, Inorganic phases, Inter. Ctr. Diffraction Data, 1992.

**Figure captions**

Fig. 1.     Absorption spectra of uranium ion in 6.9 M $CaCl_2$ (curve 1) and 1 M $HClO_4$

            (curve 2) at 298 K.

Fig. 2.     Raman spectra of uranium ion in 1 M $HClO_4$ (curve 1) and 6.9 M $CaCl_2$

            (curve 2) at 298 K.

Fig. 3      Cyclic voltammogram for the redox reaction of $UO_2^{2+}$ in 6.9 M $CaCl_2$ at 298

            K. Concentration of $UO_2^{2+}$; 0.05 M, working electrode; platinum rod of 2

            mm$\phi$, potential scanning rate; from 0.005 to 0.2 V s$^{-1}$.

Fig. 4      Cyclic voltammograms for the redox reaction of $UO_2^{2+}$ in 6.9 M $CaCl_2$ at

17

298 K. Concentration of $UO_2^{2+}$; 0.05 M, working electrode; platinum rod of 2 mmϕ, potential scanning rate; 0.1 V s$^{-1}$, potential scanning range; from –0.15 to 0.7 V (curve 1), from –0.3 to 0.7 V (curve 2), from –0.4 to 0.7 V (curve 3) and from –0.5 to 0.7 V (curve 4), from –0.6 to 0.7 V (curve 5), and from –0.7 to 0.7 V (curve 6), respectively.

Fig. 5    Cyclic voltammogram for the redox reaction of $UO_2^{2+}$ in 6.9 M $CaCl_2$ at 298 K. Concentration of $UO_2^{2+}$; 0.05 M, working electrode; glassy carbon rod of 5 mmϕ, potential scanning rate; from 0.01 to 0.2 V s$^{-1}$.

Fig. 6    Photo of the electrolytic deposit of uranium oxide.

Fig. 7    SEM micrograph of the electrolytic deposit of uranium (a) and $UO_2$ powder (b).

Fig. 8    X-ray diffraction analysis of the electrolytic deposit of uranium (curve 1) and $UO_2$ powder (curve 2). The asterisk "*" indicates the peak of $UO_2$ crystal based on the database.

Fig. 9    Absorption spectra of $UO_2Cl_2$ in 6.9 M $CaCl_2$ before and after electrolysis.

Fig. 10    Cyclic voltammograms for the redox of the $UO_2^{2+}$ in 6.9 M $CaCl_2$ (curve 1), 6.2 M (curve 2), 5.6 M (curve 3), 5.1 M (curve 4), 4.7 M (curve5), and 3.3 M

(curve 6), respectively.
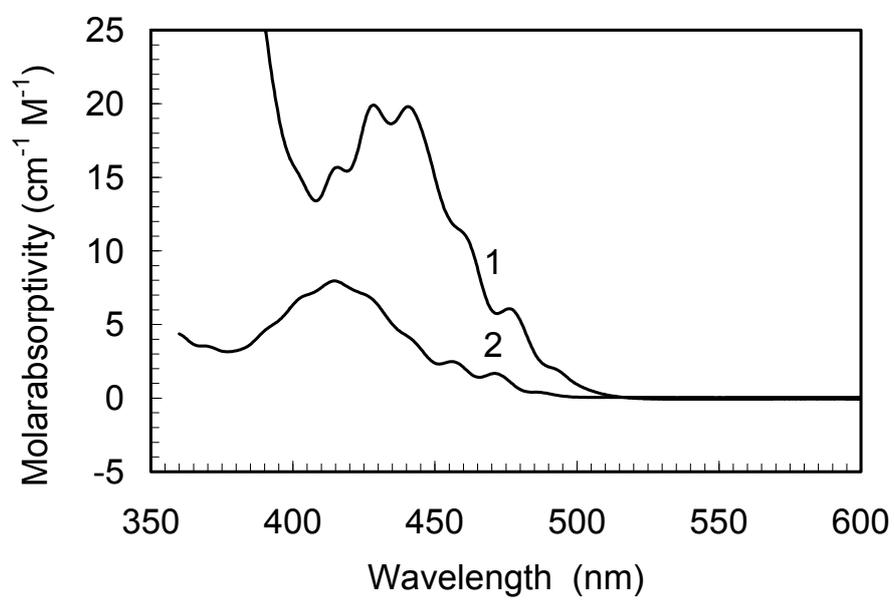
Fig. 1, Uehara, et al.,

Fig. 2, Uehara, et al.,

I (mA cm⁻²) axis labels: 2, 0, -2, -4

E (V vs. Ag|AgCl) axis labels: -0.5, 0, 0.5

Curve labels: $I_{a,1}$, $I_{a,2}$, $I_{c,1}$

0.005
0.01
0.02
0.05
0.1
0.2
V s⁻¹
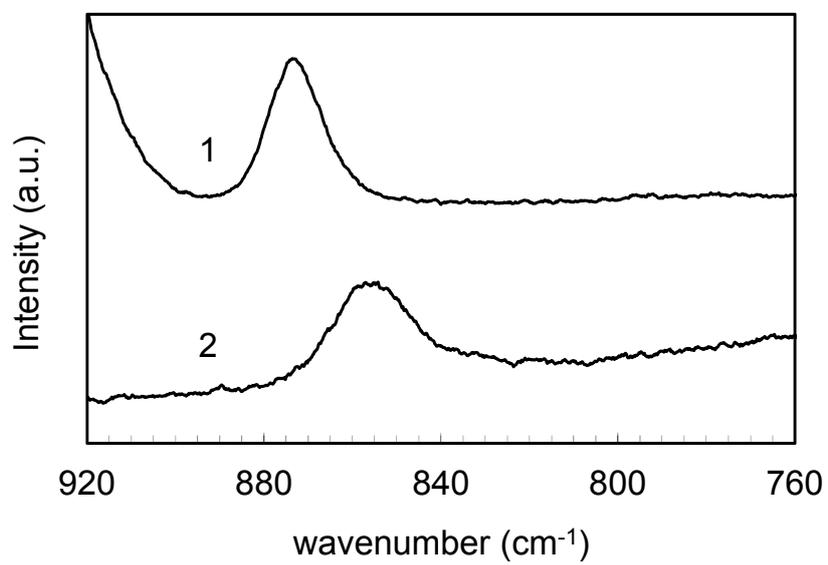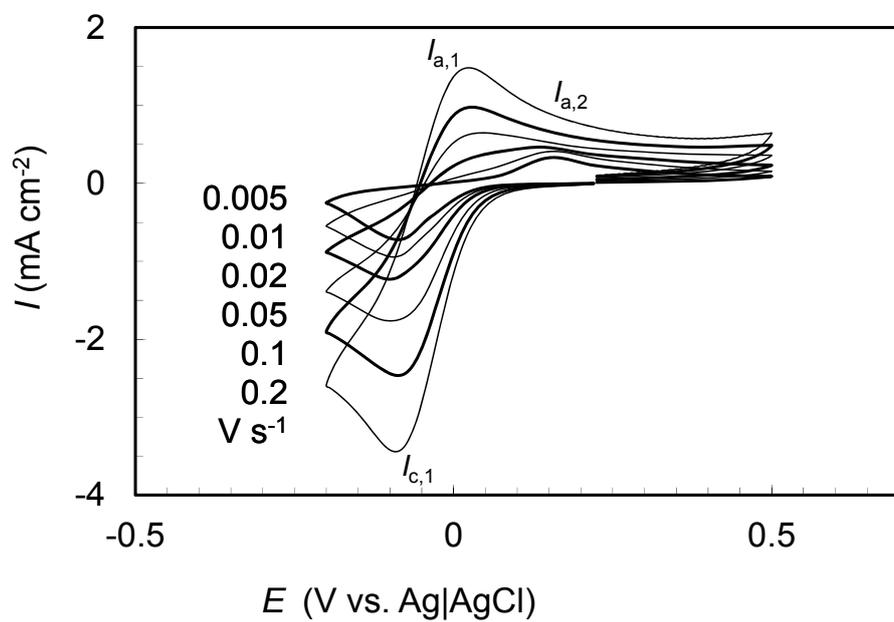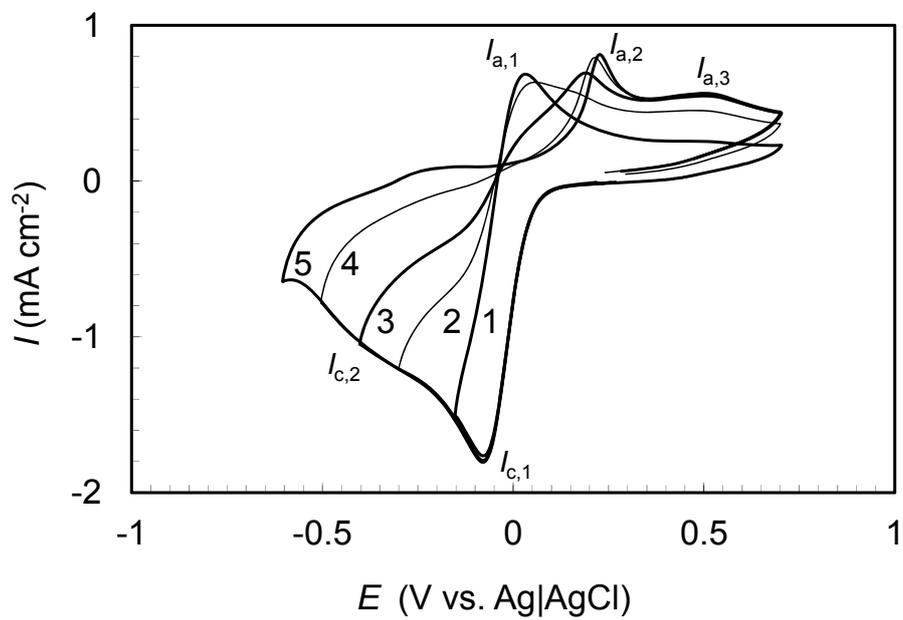
Fig. 3, Uehara, et al.,

Fig. 4, Uehara, et al.,
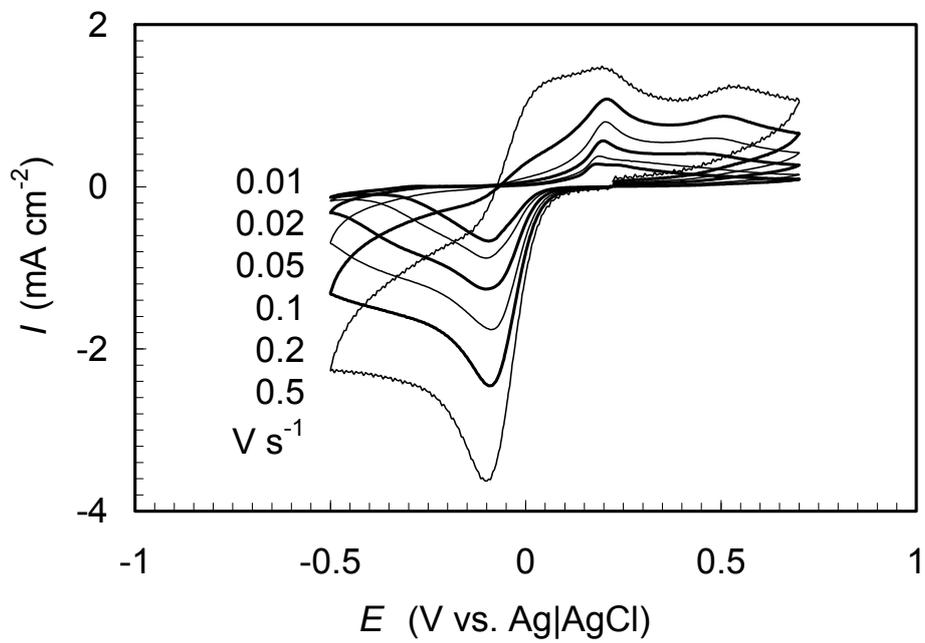
Fig. 5, Uehara, et al.,

Fig. 6, Uehara, et al.,
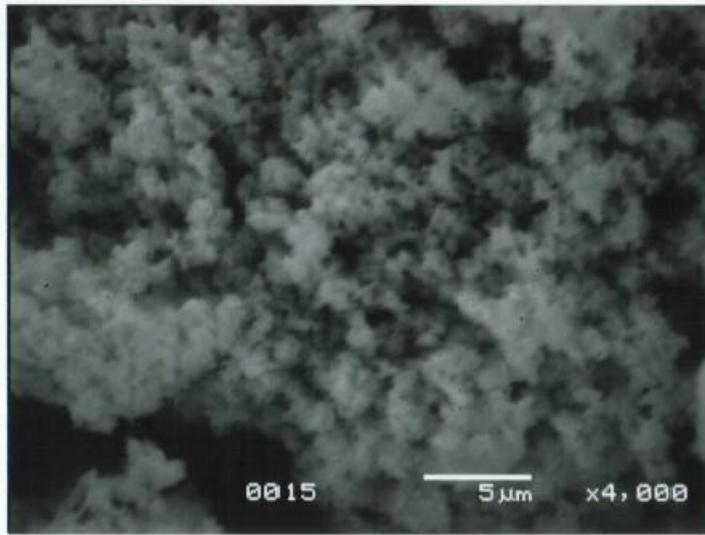
(a)



(b)

Fig. 7, Uehara, et al.,

26

Fig. 8, Uehara, et al.,

Fig. 9, Uehara, et al.,

$I$ (mA cm$^{-2}$)

$E$ (V vs. Ag|AgCl)

1
2
3
4
5
6

Fig. 10, Uehara, et al.,